Journal of Experimental Botany, Vol. 64, No. 8, pp. 2269–2281, 2013
doi:10.1093/jxb/ert086 Advance Access publication 5 April, 2013
This paper is available online free of all access charges (see http://jxb.oxfordjournals.org/open_access.html for further details)

Journal of Experimental Botany
www.jxb.oxfordjournals.org

RESEARCH PAPER

Importance of leaf anatomy in determining mesophyll diffusion conductance to CO_2 across species: quantitative limitations and scaling up by models

Magdalena Tomás[1], Jaume Flexas[1]*, Lucian Copolovici[2], Jeroni Galmés[1], Lea Hallik[2], Hipólito Medrano[1], Miquel Ribas-Carbó[1], Tiina Tosens[2], Vivian Vislap[2] and Ülo Niinemets[2]

[1] Grup de Recerca en Biologia de les Plantes en Condicions Mediterrànies. IMEDEA—Universitat de les Illes Balears, Carretera de Valldemossa Km.7.5, 07122 Palma de Mallorca, Spain
[2] Institute of Agricultural and Environmental Sciences, Estonian University of Life Sciences, Kreutzwaldi 1, Tartu 51014, Estonia

* To whom correspondence should be addressed. Email: jaume.flexas@uib.es

Received 16 January 2013; Revised 26 February 2013; Accepted 1 March 2013

Abstract

Foliage photosynthetic and structural traits were studied in 15 species with a wide range of foliage anatomies to gain insight into the importance of key anatomical traits in the limitation of diffusion of CO_2 from substomatal cavities to chloroplasts. The relative importance of different anatomical traits in constraining CO_2 diffusion was evaluated using a quantitative model. Mesophyll conductance (g_m) was most strongly correlated with chloroplast exposed surface to leaf area ratio (S_c/S) and cell wall thickness (T_{cw}), but, depending on foliage structure, the overall importance of g_m in constraining photosynthesis and the importance of different anatomical traits in the restriction of CO_2 diffusion varied. In species with mesophytic leaves, membrane permeabilities and cytosol and stromal conductance dominated the variation in g_m. However, in species with sclerophytic leaves, g_m was mostly limited by T_{cw}. These results demonstrate the major role of anatomy in constraining mesophyll diffusion conductance and, consequently, in determining the variability in photosynthetic capacity among species.

Key words: cell wall thickness, diffusion model, leaf anatomy, leaf structure, photosynthesis, quantitative photosynthetic limitations.

Abbreviations: α, leaf absorptance; β, fraction of absorbed light that reaches photosystem II; Γ^*, CO_2 compensation point in the absence of mitochondrial respiration; Φ_{PSII}, effective quantum efficiency of the PSII photochemistry; ΔL_{ias}, effective diffusion path length in the gas phase; ϵ_{PSII}, fraction of electrons absorbed by PSII; ς, diffusion path tortuosity; A_{mass}, photosynthetic capacity per dry mass; A_N, net CO_2 assimilation rate; C_a, atmospheric CO_2 concentration; C_c, chloroplastic CO_2 concentration; C_i, substomatal CO_2 concentration; C_i-C_c, CO_2 drawdown from intercellular airspace to chloroplasts; D_a, diffusion coefficient for CO_2 in the gas phase; D_L, leaf density; D_w, aqueous phase diffusion coefficient for CO_2; f_{ias}, volume fraction of intercellular air spaces; F_m', maximum fluorescence in light-adapted state; F_s, steady-state fluorescence emission; g_{cel}, partial liquid phase conductance for different portions along cell walls; g_{cyt}, cytosol conductance; g_{env}, chloroplast envelope conductance; g_{ias}, intercellular air space conductance to CO_2 (gas phase conductance); g_{liq}, sum of liquid and lipid phase conductances; g_m, mesophyll diffusion conductance; g_{pl}, plasma membrane conductance; g_s, stomatal conductance to CO_2; g_{tot}, total conductance to CO_2 from ambient air to chloroplasts; $H/(RT_k)$, dimensionless form of Henry's law constant; J_F, linear electron transport rate from chlorophyll fluorescence; J_{max}, maximum photosynthetic electron transport rate; K_c, Michaelis–Menten constant for the carboxylation activity of Rubisco; K_o, Michaelis–Menten constant for the oxygenation activity of Rubisco; l_b, biochemical limitation; L_{chl}, length of chloroplasts exposed to intercellular air spaces; L_{cyt}, diffusion pathway length in the cytoplasm; l_{ias}, gas-phase limitation; l_m, mesophyll limitation; l_s, stomatal limitation; M_A, leaf mass per area; O, leaf internal oxygen concentration; p_i, effective porosity in the given part of the diffusion pathway; Q, incident quantum flux density; R, gas constant; R_d, leaf respiration in the dark; $r_{f,i}$, proportional reduction of D_w in the cytosol and in the stroma compared with free diffusion in water; R_L, leaf respiration in the light; $S_{C/O}$, Rubisco specificity factor; S_c/S, chloroplast surface area exposed to intercellular air spaces per unit of leaf area; S_c/S_m, ratio of exposed chloroplasts to mesophyll surface areas; S_m/S, mesophyll surface area exposed to intercellular air spaces per unit of leaf area; S_s, cross-sectional area of mesophyll cells in micrograph; SE, standard error; T_{chl}, chloroplast thickness; T_{cw}, cell wall thickness; T_{cyt}, cytoplasm thickness; T_k, absolute temperature; T_L, leaf thickness; t_{mes}, mesophyll thickness; V_{cmax}, maximum rates for the carboxylation activity of Rubisco; W, width of the leaf anatomical section.

Introduction

Leaf anatomical characteristics are key functional and adaptive traits determining plant capacity to thrive in specific environments, in particular, because these traits also have important implications for foliage potential photosynthesis (Niinemets *et al.*, 2009a; Scafaro *et al.*, 2011; Terashima *et al.*, 2011). Analysis of global variations in leaf functional traits—the leaf economics spectrum—has established that the variation in leaf dry mass per area (M_A) is strongly associated with other key leaf traits such as maximum photosynthetic capacity per dry mass (A_{mass}), leaf life span, nitrogen and phosphorous contents per dry mass, and respiration (Wright *et al.*, 2004). Species with lower M_A present short leaf life spans, high photosynthetic capacities and nutrient contents, and low leaf area construction costs, resulting in fast growth in environments with high availability of resources. In contrast, species with higher M_A and lower A_{mass} present the opposite suite of traits and have higher cost for leaf area formation, particularly due to investment in vasculature and cell walls (Niinemets *et al.*, 2007; Hikosaka & Shigeno, 2009) and overall improved resistance to low fertility and drought, but low growth rates (Niinemets, 2001; Wright *et al.*, 2004). It has been hypothesized that the negative relationship between M_A and photosynthetic capacity is partly because of greater biomass investment in support tissues and cell wall thickening involving stronger CO_2 diffusion limitations to photosynthesis (Niinemets, 1999; Wright *et al.*, 2004; Niinemets *et al.*, 2007)

Mesophyll conductance to CO_2 (g_m) is the measure of the CO_2 diffusion facility from substomatal cavities to the sites of carboxylation in the chloroplasts (Flexas *et al.*, 2008, 2012) Mesophyll conductance is finite and variable and plays a major role in constraining photosynthetic productivity (Niinemets *et al.*, 2009a). Large differences in g_m have been shown between and within species with different leaf forms and habits (Flexas *et al.*, 2008; Warren, 2008; Niinemets *et al.*, 2009a, 2011). Whilst rapid changes of g_m in response to environmental drivers probably depend on biochemical factors such as changes in the permeability of membranes to CO_2 facilitated by cooporins (Hanba *et al.*, 2004; Flexas *et al.*, 2006, 2012), maximum values of g_m for a given species or genotype are suggested to be related to leaf anatomical properties (Niinemets *et al.*, 2009a; Tosens *et al.*, 2012a). In particular, it has been shown that leaves with a more robust structure and higher M_A exhibit lower photosynthetic rates due to large CO_2 drawdown from substomatal cavities (C_i) to chloroplasts (C_c), C_i-C_c, demonstrating that the photosynthetic capacity is limited by g_m (Flexas *et al.*, 2008, Niinemets *et al.*, 2009a). Therefore, understanding the structural and physiological basis of variation in g_m is crucial for understanding photosynthetic controls in natural ecosystems and for breeding of plant cultivars with improved photosynthetic characteristics.

At the leaf level, two components of M_A—leaf thickness and density—have been proposed to exert opposite effects on setting the maximum g_m, with increases in thickness increasing g_m and increases in density reducing it (Niinemets *et al.*, 2009b, Hassiotou *et al.*, 2010). Inside leaves, the CO_2 diffusion pathway consists of two phases, an intercellular gas phase and a cellular liquid phase, the latter consisting of aqueous and lipid components(Niinemets and Reichstein, 2003b; Evans *et al.*, 2009). The gas phase pathway through intercellular air spaces is assumed to have a smaller effect on the overall diffusion limitations than the components of the liquid phase (Evans *et al.*, 2009). This was confirmed in several studies comparing CO_2 diffusion in air and helox—air where helium replaces nitrogen to increase diffusivity—showing that the diffusion in the intercellular gas phase had little effect on photosynthesis (Parkhurst and Mott, 1990) The cellular phase is composed of the cell wall, plasma membrane, cytosol, and chloroplast envelopes and stroma. Among these components, the cell walls and chloroplast envelope have been suggested to limit g_m most severely (Terashima *et al.*, 2011). Accordingly, several reports have shown positive correlations between g_m and the surface of chloroplasts adjacent to intercellular air spaces (S_c/S), which is sometimes considered as the most important anatomical trait affecting g_m (Evans *et al.*, 1994; Terashima *et al.*, 2006; Tholen *et al.*, 2008). However, some estimates suggest that differences in cell wall thickness (T_{cw}) can explain as much as 25–50% of the variability in g_m (Evans *et al.*, 2009; Terashima *et al.*, 2011; Tosens *et al.*, 2012b). Negative correlations between g_m and T_{cw} have been shown when comparing Australian *Banksia* species (Hassiotou *et al.*, 2010), rice relatives (Scafaro *et al.*, 2011), Eastern Australian species with varying anatomy (Tosens *et al.*, 2012b), and Mediterranean *Abies* species (Peguero-Pina *et al.*, 2012). Recently, Terashima *et al.* (2011) showed that $g_m/(S_c/S)$ decreases with increasing T_{cw}, i.e. the relative influence of the exposed chloroplast surface in setting the maximum g_m is variable, and that this variation can potentially be explained by variations in T_{cw}.

Few previous studies have quantitatively addressed the influence of leaf anatomical traits on the diffusion of CO_2, and these studies have focused only on a few species and specific parts of the CO_2 diffusion pathway (Evans *et al.*, 1994; Terashima *et al.*, 2006; Hassiotou *et al.*, 2010; Scafaro *et al.*, 2011; Peguero-Pina *et al.*, 2012; Tosens *et al.*, 2012b). Hence, the whole diffusion pathway of CO_2 from the substomatal cavities to the chloroplasts has not been quantitatively linked to g_m in plants with widely varying leaf structures and photosynthetic capacities. Furthermore, the overall importance of g_m in constraining the photosynthetic rate in species with different foliage architecture has not been characterized. To fill this gap, we aimed with the present study: (i) to analyse the role of different components of the diffusion pathway across a wide range of foliage architectures and leaf photosynthetic capacities; (ii) to associate the interspecific differences in leaf anatomy with the integrated leaf architectural traits such as M_A and g_m; (iii) to quantify the distribution of overall photosynthetic limitation among biochemistry, mesophyll diffusion, and stomata; and (iv) to quantify the resistance that each anatomical component exerts on the diffusion of CO_2 inside the leaf.

Material and methods

Plant material

Fifteen taxa of different growth form and leaf longevity were selected for the study to obtain an extensive range of variation in leaf morphology and anatomy (Supplementary Table S1 at *JXB* online). Five

species were annual herbs (*Capsicum annuum*, *Helianthus annuus*, *Phaseolus vulgaris*, *Spinacea oleracea*, *Ocimum basilicum*) and the rest were broad-leaved trees: four deciduous (*Acer negundo*, *Alnus subcordata*, *Betula pubescens*, *Catalpa speciosa*), one semi-deciduous (*Quercus brantii*) and five evergreens (*Quercus ilex*, *Citrus reticulata*, *Ficus elastica*, *Pittosporum tobira*, *Washingtonia filifera*). All species were dicots, except for the palm *Washingtonia filifera.*

All plants were grown either from commercial seed or from seeds collected in the field, except for *F. elastica* where rooted cuttings of a single mother plant were used. The plants were grown in a growth room with a 10 h photoperiod, a day/night temperature of 24/18 °C, 60% air humidity, and a constant photon flux density of 350 µmol m^{-2} s^{-1} at plant level provided by Philips HPI-T Plus 400 W metal halide lamps. The daily integrated incident quantum flux density was 12.6 mol m^{-2} d^{-1}. The growth substrate was a 1/1 mix of quartz sand and standard potting soil (Biolan Oy, Finland) including slow-release NPK (3/1/2 ratio) fertilizer with microelements, and the plants were irrigated daily to soil field capacity. The size of the pots varied between 1 and 5 l depending on plant age and size. In all cases, fully developed young (current-season leaves in evergreens) leaves were used for the measurements. In herbs, the plants were measured 1 month after seed germination, whilst woody species were measured on the second growing year. All physiological and structural analyses were replicated with at least three independent plants per taxa.

Foliage gas exchange and fluorescence measurements

Attached leaves were used for simultaneous leaf gas-exchange and chlorophyll-fluorescence measurements using a portable gas exchange fluorescence system GFS-3000 (Walz, Effeltrich, Germany) equipped with a leaf chamber fluorometer with an 8 cm^2 cuvette window area. Light was provided by the LED light source of the leaf chamber fluorometer (10% blue and 90% red light) and the humidity was controlled by a built-in GFS-3000 humidifier. Use of a certain fraction of blue light is routinely used in portable photosynthesis devices to induce stomatal opening. Although blue light is absorbed more strongly by the upper leaf layers and may lead to discrepancies among photosynthesis and fluorescence profiles (Evans and Vogelmann, 2006), thereby altering g_m estimations by the combined gas-exchange/fluorescence techniques (Loreto *et al.*, 2009), the amount of blue light used in our study was small and the expected effect minor.

The standard conditions for leaf stabilization in the cuvette were: leaf temperature of 25 °C, saturating quantum flux density of 1500 µmol m^{-2} s^{-1}, and CO_2 concentration in the cuvette (C_a) of 385 µmol CO_2 mol air^{-1}. Once the steady-state conditions were reached, typically 15–20 min after clamping the leaf in the cuvette, CO_2 response curves of net assimilation (A_N) were measured. First, C_a was lowered stepwise from 385 to 50 µmol CO_2 mol air^{-1} and then raised again to 385 µmol CO_2 mol air^{-1}, and the leaf was kept at this C_a until the original A_N value was achieved. Next, C_a was increased stepwise from 385 to 1500 µmol CO_2 mol air^{-1} and returned again to 385 µmol CO_2 mol air^{-1}. In all cases, measurements of A_N and steady-state fluorescence yield (F_s) were recorded after the gas-exchange rates stabilized at the given C_a. After recording the A_N value, a flash of saturating white light was given to determine the maximum fluorescence yield in light-adapted state (F_m'). After completion of the CO_2 response curves, the light was switched off and respiration rate in the dark (R_d) was determined. In calculations of A_N, R_d, and intercellular CO_2 concentration (C_i), corrections for the diffusion leakage of CO_2 into and out of the leaf chamber were included as described by Flexas *et al.* (2007).

Measurements of leaf optical properties

Leaf transmittance and reflectance measurements were conducted with a spectrometer (AvaSpec-2048-2; Avantes, Apeldoorn, The Netherlands) using an integrating sphere (ISP-80-8-R; Ocean Optics, Dunedin, FL, USA). Leaf absorptance (α) was calculated as 1 minus the sum of reflectance and transmittance. Three leaves of each species were measured, and within each leaf, three replicate measurements were made. Average absorptance across the 400–700 nm region was used to characterize the fraction of incident photosynthetically active radiation absorbed by the leaf.

Anatomical measurements

After the gas-exchange measurements, 1 × 1 mm pieces were cut between the main veins from the same leaves for anatomical measurements. Leaf material was quickly fixed under vacuum with 4% glutaraldehyde and 2% paraformaldehyde in 0.1 M phosphate buffer (pH 7.2). Afterwards, the samples were fixed in 1% osmium tetroxide for 1 h and dehydrated in a graded ethanol series, followed by washing three times in propylene oxide. The dehydrated segments were embedded in Spurr's resin (Monocomp Instrumentación, Madrid, Spain) and cured in an oven at 60 °C for 48 h. Semi-thin (0.8 µm) and ultrathin (90 nm) cross-sections were cut with an ultramicrotome (Reichert & Jung model Ultracut E). Semi-thin cross-sections were stained with 1% toluidine blue and viewed under an Olympus BX60light microscope. Photos were taken at 200× and 500× magnification with a digital camera (U-TVO.5XC; Olympus) to measure the leaf thickness and thickness of the palisade and spongy tissue layers (Supplementary Fig. S1A–C). Ultrathin cross-sections for transmission electron microscopy (TEM H600; Hitachi) were contrasted with uranyl acetate and lead citrate. Photos were taken at 2000× magnification (Supplementary Fig. S1D–F) to measure the length of mesophyll cells and chloroplasts adjacent to intercellular air spaces and chloroplast width and thickness, and the volume fraction of intercellular air space calculated as:

$$f_{ias} = 1 - \frac{\sum S_s}{t_{mes} W} \quad (1)$$

where ΣS_s is the total cross-sectional area of mesophyll cells, W is the width of the section, and t_{mes} is the mesophyll thickness between the two epidermises. Mesophyll (S_m/S) and chloroplast (S_c/S) surface area exposed to intercellular air spaces per leaf area were calculated separately for spongy and palisade tissues as described by Evans *et al.* (1994) and Syvertsen *et al.* (1995). The curvature correction factor was measured and calculated for each species according to Thain (1983) for palisade and spongy cells by measuring their width and height and calculating an average width/height ratio. The curvature factor correction ranged from 1.16 to 1.4 for spongy cells and from 1.4 to 1.5 for palisade cells. All parameters were analysed at least in four different fields of view and at three different sections. Weighted averages based on tissue volume fractions were calculated for S_m/S and S_c/S.

T_{cw} and cytoplasm thickness (T_{cyt}) were measured at 20 000–40 000× magnification depending on the species (Supplementary Fig. S1G–I). Three different sections per species and four to six different fields of view were measured for each anatomical characteristic. Micrographs were selected randomly in each section and T_{cw} was measured for two to three cells per micrograph. Ten measurements for spongy tissue and ten for palisade parenchyma cells were made for each anatomical trait, and weighted averages based on tissue volume fractions were calculated. All images were analysed with Image analysis software (ImageJ; Wayne Rasband/NIH, Bethesda, MD, USA).

M_A and leaf density

The leaves were scanned at 300 dpi, and then oven dried at 70 C for 48 h and their dry mass was estimated. Leaf area was determined from the images with Image J. From these measurements, M_A was calculated. Using the estimates of leaf thickness from anatomical

measurements, leaf density (D_L) was calculated as M_A per unit leaf thickness (Niinemets, 1999).

Estimation of g_m and model parameters Farquhar et al. (1980) by combined gas-exchange/fluorescence method

The chloroplastic hypothetical CO_2 compensation point (Γ*) in the absence of R_d was calculated from the Rubisco specificity factor ($S_{C/O}$) as:

$$\Gamma^* = 0.5\ O/SC/O \quad (2)$$

using the average values for $S_{C/O}$ reported by Galmés *et al.* (2005) for each different leaf habit (Supplementary Table S2 at *JXB* online). A sensitivity analysis showed that the precise value of Γ* within the reported range did not significantly affect the g_m estimates (Supplementary Table S3A at *JXB* online).

From chlorophyll fluorescence measurements, the actual photochemical efficiency of photosystem II (Φ_{PSII}) was determined from F_s and the maximum fluorescence yield during a light-saturating pulse of 4500 µmol m^{-2} s^{-1} (F_m') following the method of Genty *et al.* (1989):

$$\Phi_{PSII} = (F_m' - F_s)/F_m' \quad (3)$$

The linear electron transport rate on the basis of chlorophyll fluorescence (J_F) was then calculated as:

$$J_F = \Phi_{PSII} Q \alpha \varepsilon_{PSII} \quad (4)$$

where Q is the photosynthetically active quantum flux density, α is the leaf absorptance, and ε_{PSII} is the fraction of light absorbed by PSII. As routinely assumed, ε_{PSII} was taken as 0.5 (Loreto *et al.*, 1994; Niinemets *et al.*, 2005).

Furthermore, the g_m to CO_2 was estimated according to Harley *et al.* (1992) as:

$$g_m = \frac{A_N}{C_i - \frac{\Gamma^*(J_F + 8(A_N + R_L))}{J_F - 4(A_N + R_L)}} \quad (5)$$

where R_L is the respiration rate in the light. In this study, R_d was used as a proxy for R_L (Gallé *et al.*, 2009). In other studies, half R_d has been used (Piel *et al.*, 2002; Niinemets *et al.*, 2005). However, as shown in Supplementary Table S3B, no significant differences in g_m were found when using the proxy for R_L, and hence we concluded that selection of the appropriate value for R_L is not a critical issue for our g_m estimates, confirming a previous sensitivity analysis (Niinemets *et al.*, 2006).

The obtained values of g_m were used to transform the A_N-C_i response curves into A_N versus C_c response curves as $C_c = C_i - A_N/g_m$. Finally, Farquhar *et al.* (1980) model parameters, the maximum velocity of carboxylation (V_{cmax}) and the capacity for photosynthetic electron transport (J_{max}) on the basis of C_c were calculated according to Bernacchi *et al.* (2002). Three replicates estimates of g_m were available for every species.

Estimation of g_m from gas exchange measurements only: the curve-fitting method

The curve-fitting method introduced by Ethier and Livingston (2004) as applied by Niinemets *et al.* (2005) was used to obtain an alternative estimate of g_m. This method is based on changes in the curvature of A_N versus C_i response curves due to finite g_m such that the Farquhar *et al.* (1980) model based on C_i imperfectly fits the data (Ethier and Livingston 2004). Thus, including g_m as a fitted parameter significantly improves the model fit. Estimates of J_{max}, V_{cmax}, and g_m were derived from fitting A_N-C_i curves as previously described. Values of the Michaelis–Menten constant for CO_2 (K_c), and oxygen (K_o) and their temperature responses used for these estimations were from Bernacchi *et al.* (2002). Γ* was calculated according to Eqn 2, and R_d by gas exchange measurements at 385 µmol CO_2 mol air^{-1}. At least three plants per species were used to estimate g_m. The same leaves were used for estimation of g_m by the Ethier and Livingston (2004) and Harley *et al.* (1992) methods.

g_m modelled from anatomical characteristics

The one-dimensional gas diffusion model of Niinemets and Reichstein (2003a) as applied by Tosens *et al.* (2012a) was employed to estimate the share of different leaf anatomical characteristics in determining g_m. g_m as a composite conductance for within-leaf gas and liquid components is given as:

$$g_m = \frac{1}{\frac{1}{g_{ias}} + \frac{RT_k}{H \cdot g_{liq}}}, \quad (6)$$

where g_{ias} is the gas phase conductance inside the leaf from substomatal cavities to outer surface of cell walls, g_{liq} is the conductance in liquid and lipid phases from outer surface of cell walls to chloroplasts, R is the gas constant (Pa m^3 K^{-1} mol^{-1}), T_k is the absolute temperature (K), and H is the Henry's law constant (Pa m^3 mol^{-1}). g_m is defined as a gas-phase conductance, and thus $H/(RT_k)$, the dimensionless form of Henry's law constant, is needed to convert g_{liq} to corresponding gas-phase equivalent conductance (Niinemets and Reichstein, 2003a). In the model, the gas-phase conductance (and the reciprocal term, r_{ias}) is determined by average gas-phase thickness, ΔL_{ias}, and gas-phase porosity, f_{ias} (fraction of leaf air space):

$$g_{ias} = \frac{1}{r_{ias}} = \frac{D_a \cdot f_{ias}}{\Delta L_{ias} \cdot \varsigma} \quad (7)$$

where is the diffusion path tortuosity (m m^{-1}) and D_a (m^2 s^{-1}) is the diffusion coefficient for CO_2 in the gas phase (1.51×10^{-5} at 25 °C). ΔL_{ias} was taken as half the mesophyll thickness. The partial determinants of the liquid-phase diffusion pathway (the reciprocal term r_i, where i stands either for cell wall, cytosol, or stroma conductance) were calculated as:

$$g_i = \frac{1}{r_i} = \frac{r_{f,i} \cdot D_w \cdot p_i}{\Delta L_i} \quad (8)$$

where ΔL_i (m) is the diffusion path length in the corresponding component of the diffusion pathway, p_i (m^3 m^{-3}) is its effective porosity, and D_w is the aqueous phase diffusion coefficient for CO_2 (1.79×10^{-9} m^2 s^{-1} at 25 °C). The dimensionless factor $r_{f,i}$ accounts for the reduction of D_w compared with free diffusion in water, and was taken as 1.0 for cell walls (Rondeau-Mouro *et al.*, 2008) and 0.3 for cytosol and stroma (Niinemets and Reichstein, 2003b). In addition, $r_{f,i}$ values for cytosol and stroma were estimated using a least-squares iterative analysis to assess the sensitivity of g_m to values of $r_{f,i}$ (Supplementary Figs S2 and S3 at *JXB* online). In this analysis, $r_{f,i}$ was allowed to vary between 1 and 0.05, and the values of $r_{f,i}$ were varied within this range to minimize the difference between measured and modelled g_m. Whilst this approach improved the agreement between modelled and measured g_m, the extreme values obtained for $r_{f,i}$ seemed unrealistic (Supplementary Figs S2 and S3). p_i was set to 1.0 for cytosol and stroma. There are no direct measurements of cell wall porosity, but it has been suggested that this parameter might vary with T_{cw} among species (Terashima *et al.*, 2006; Evans *et al.*, 2009; Tosens *et al.*, 2012b). Therefore, given the heterogeneous

series of species used in this experiment, p_i was estimated using a least-squares iterative analysis assuming a hypothetical relationship between porosity and T_{cw} as described by Tosens *et al.* (2012b). Again, a least-squares iterative approach was employed to get the best fit between measured and modelled g_m. The p_i range in this analysis was fixed at 0.028 (Tosens *et al.*, 2012b) for the thickest to 0.3 (Nobel, 1991) for the thinnest cell walls (Supplementary Table S5 at *JXB* online). We used an estimate of 0.0035 m s^{-1} for both plasma membrane conductance (g_{pl}) and chloroplast envelope conductance (g_{env}) as previously suggested (Evans *et al.*, 1994; Tosens *et al.*, 2012a).

Carbonic anhydrase in cytosol and chloroplasts could facilitate the diffusion of CO_2 through the liquid phase. However, there is little evidence for the involvement of carbonic anhydrase in g_m and A_N (reviewed by Flexas *et al.*, 2008, 2012). Therefore, following Tosens *et al.* (2012a), we did not include the potential effect of carbonic anhydrase in our analysis.

In previous studies, we scaled the total liquid-phase diffusion conductance by S_c/S ratio (Tosens *et al.*, 2012a) that determines the number of parallel diffusion pathways from outer surfaces of cell walls to chloroplasts.

$$g_{liq} = \frac{S_c}{\left(r_{cw} + r_{pl} + r_{cyt} + r_{en} + r_{st}\right) S} \tag{9}$$

Although, cell wall and plasmalemma resistances actually scale with the S_m/S ratio, use of S_c/S has been deemed to be appropriate, as S_c/S is generally close to the S_m/S ratio (Scafaro *et al.*, 2011; Peguero-Pina *et al.*, 2012), i.e. there is little cell wall area free of chloroplasts. Even if S_c/S is significantly smaller than S_m/S, the cytosolic distance between the neighbouring chloroplasts is generally large and this can still constrain the diffusion flux in interchloroplastial areas of cell wall (locally large cytosol conductance, g_{cyt}; Fig. 1). However, the significance of the r_{cyt} depends on the other parts of the diffusion pathway as well.

To explicitly assess the importance of diffusion of CO_2 through interchloroplastial areas, we considered two different pathways of CO_2 inside the cell, one for cell wall parts with chloroplasts and the other for interchloroplastial areas as described by Tholen *et al.* (2012). For exposed cell wall portions lined with chloroplasts, the partial liquid phase conductance, $g_{cel,1}$, inside the cell is given as:

$$g_{cel,1} = \frac{1}{r_{cyt,1} + r_{env} + r_{st,1}} \tag{10}$$

where $r_{cyt,1}$ and $r_{st,1}$ are cytosolic resistance from the plasmalemma inner surface to the outer surface of chloroplasts and the stromal resistance in the direction perpendicular to cell wall (Fig. 1), respectively, both calculated by Eqn 8. For $r_{cyt,1}$, the diffusion pathway length, $\Delta L_{cyt,1}$, is given as the average distance between the chloroplasts and cell wall in cell wall areas lined by chloroplasts (Fig. 1), whilst for $r_{st,1}$, ΔL_i, was taken as half of the chloroplast thickness, $\Delta T_{chl}/2$. For the cell wall portions without chloroplasts, the partial conductance, $g_{cel,2}$, is given analogously as:

$$g_{cel,2} = \frac{1}{r_{cyt,2} + r_{env} + r_{st,2}} \tag{11}$$

where $r_{cyt,2}$ is the cytosolic resistance from interchloroplastic cell wall portions towards the chloroplast and $r_{st,2}$ is the stromal conductance in a direction parallel with the cell wall (Fig. 1). The diffusion path length for $r_{cyt,2}$ (Eqn), $\Delta L_{cyt,2}$, is driven both by the distance between the neighbouring chloroplasts, chloroplast thickness, and chloroplast distance from the cell wall and was approximated as:

$$\Delta L_{cyt,2} = \sqrt{\left(\frac{\Delta T_{chl}}{2} + \Delta L_{cyt,1}\right)^2 + \left(\frac{\Delta L_{chl}}{2}\right)^2} \tag{12}$$

where ΔL_{chl} is the distance between the neighbouring chloroplasts. $\Delta L_{cyt,2}$ was calculated as a harmonic average, which more correctly represents the diffusion pathway of $r_{cyt,2}$. Finally, the diffusion pathway length for $r_{st,2}$ was taken as a quarter of the chloroplast length.

Considering further that the fraction of exposed cell wall area lined with chloroplasts is given by S_c/S_m and the fraction free of chloroplasts as $1 - S_c/S_m$, the total cellular conductance (sum of parallel conductances) is given as:

$$g_{cel,tot} = \frac{S_c}{S_m} g_{cel,1} + \left(1 - \frac{S_c}{S_m}\right) g_{cel,2} \tag{13}$$

Total liquid phase conductance from the outer surface of cell walls to carboxylation sites in the chloroplasts is the sum of serial conductances in the cell wall, plasmalemma, and inside the cell:

$$g_{liq} = \frac{S_m}{\left(r_{cw} + r_{pl} + r_{cel,tot}\right) S} \tag{14}$$

Alternatively, the total cellular diffusion pathway can be considered to consist of two parallel pathways from the outer surface of the cell walls to the chloroplasts, one pathway corresponding to the diffusion flux through cell wall areas lines with chloroplasts and the other without chloroplasts:

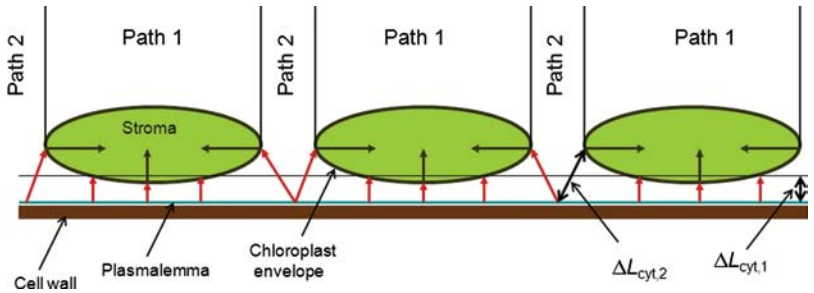

Fig. 1. Illustration of the diffusion pathway in exposed cell wall areas lined with chloroplasts (path 1) and interchloroplastial areas (path 2). The diffusion pathway in leaf lipid and liquid phases includes cell wall, plasmalemma, cytosol (shown by red arrows), chloroplast envelope membranes, and chloroplast stroma (shown by dark green arrows). The effective diffusion path length in cytosol along path 1 is taken as the average distance of chloroplasts from the cell wall, $\Delta L_{cyt,1}$, whilst the diffusion pathway length in interplastidial areas is determined by the distance between the chloroplasts and $\Delta L_{cyt,1}$ (Eqn 12).

$$g_{liq} = \frac{S_c}{\left(r_{cw} + r_{pl} + r_{cel,1}\right) S} + \frac{S_m - S_c}{\left(r_{cw} + r_{pl} + r_{cel,2}\right) S} \quad (15)$$

Although Eqns 14 and 15 are conceptually different, the values of conductances calculated by both equations were very similar, differing at most by 4%. In the current study, we have used Eqn 14.

Analysis of quantitative limitations on A_N

To separate the relative controls on A_N resulting from limited stomatal conductance (l_s), mesophyll diffusion (l_m), and limited biochemical capacity (l_b) (l_s+l_m+l_b=1), we used the quantitative limitation analysis of Jones (1985) and implemented by Grassi and Magnani, (2005). The limitations of the different components were calculated as:

$$l_s = \frac{g_{tot}/g_s \bullet \partial A_N/\partial C_c}{g_{tot} + \partial A_N/\partial C_c}, \quad (16)$$

$$l_m = \frac{g_{tot}/g_m \bullet \partial A_N/\partial C_c}{g_{tot} + \partial A_N/\partial C_c}, \text{ and} \quad (17)$$

$$l_b = \frac{g_{tot}}{g_{tot} + \partial A_N/\partial C_c}, \quad (18)$$

where g_s is the stomatal conductance to CO_2, g_m was according to Harley *et al.* (1992, Eqn 5), and g_{tot} is the total conductance to CO_2 from ambient air to chloroplasts (sum of the inverse serial conductances g_s and g_m). $\delta A_N/\delta C_c$ was calculated as the slope of A_N-C_c response curves over a C_c range of 50–100 µmol mol^{-1}. At least three curves per species were used, and average estimates of the limitations were calculated.

Quantitative analysis of partial limitations of g_m

The determinants of g_m were divided between the component parts of the diffusion pathway (Eqns 6–8). The proportion of g_m determined by limited gas-phase conductance (l_{ias}) was calculated as:

$$l_{ias} = \frac{g_m}{g_{ias}} \quad (19)$$

The share of g_m by different components of the cellular phase conductances (l_i) was determined as:

$$l_i = \frac{g_m}{g_i \frac{S_m}{S}} \quad (20)$$

where l_i is the component limitation in the cell walls, the plasmalemma, and inside the cells, and g_i refers to the component diffusion conductances of the corresponding diffusion pathways. To determine the limitations derived from the different components inside the cell (cytoplasm, chloroplast envelope, and stroma), weighted limitations of both pathways, the fraction of exposed cell wall area lined with chloroplasts and the fraction free of chloroplasts, were used.

Statistical analyses

Regression and correlation analyses were conducted using the Sigma Plot 10.0 software package (SPSS; Chicago, IL, USA). Univariate analysis of variance was performed to reveal differences between species in the studied characteristics. Differences between means were revealed by Tukey analyses (P <0.05). These analyses were performed with the IBM SPSS statistics 19.0 software package (SPSS).

Results

Leaf structural and anatomical traits

M_A varied sixfold (20–123 g m^{-2}) (Supplementary Table S4 at *JXB* online). The variation in leaf thickness was 3.7-fold with *Acer negundo* having the thinnest (123 µm) and *F. elastica* the thickest (459 µm) leaves. Spongy mesophyll thickness varied 5.2-fold, and palisade mesophyll thickness 2.5-fold (Supplementary Table S4). Generally, the palisade tissue comprised approximately 40%, and spongy tissue approximately 60% of total mesophyll, except for some species as *F. elastica* with 75% and *W. filifera* with 100% of spongy tissue. The variation in D_L was 6.4-fold with *Phaseolus vulgaris* having the least dense (0.11 g cm^{-3}) and *Q. ilex* the most dense (0.70 g cm^{-3}) leaves. M_A exhibited a significant positive correlation with D_L (Supplementary Fig. S4 at *JXB* online), but was weakly correlated with leaf thickness (r^2=0.27, P <0.05; data not shown). Therefore, the variation in M_A was mainly attributed to the leaf density.

Among the leaf ultrastructural characteristics estimated from transmission electron micrographs (Supplementary Tables S4 and S5, and Supplementary Fig. S1D–I), S_m/S varied 3.3-fold across all species (14.4–40 m^2 m^{-2}) and S_c/S varied 2.7-fold (6–19.7 m^2 m^{-2}). S_c/S_m varied between 0.31 (*Citrus reticulata*) and 0.74 (*O. basilicum*). For T_{cw} (Supplementary Fig. S1G–I), 4.8-fold variation was observed between all species (113.6–543.7 nm). Herbaceous species exhibited the thinnest cell walls together with *Catalpa speciosa*, whilst evergreens had the thickest cell walls with the maximum value of 543.7 nm observed in *Pittosporum tobira*.

Estimation of g_m with different methods

The values of g_m calculated according to the methods of Harley *et al.* (1992) and Ethier and Livingston (2004) were strongly correlated (Supplementary Fig. S5 at *JXB* online, r^2=0.80). However, the Harley *et al.*-based estimates exhibited the smallest average coefficient of variation for independent estimates within a species and therefore we report the data obtained with this method only.

Mesophyll conductance calculated by the method of Harley *et al.* (1992) varied 24-fold across all species. *H. annuus* showed the maximum values and *Citrus reticulata* the minimum values of g_m. The minimum value for the coefficient of variation in g_m was 1.9% (*Pittosporum tobira*), whilst the maximum value was 32.9% (*Q. ilex*). The average of the coefficient of variation for all species was 16.5%.

g_m in relation to physiological characteristics

Net assimilation rate correlated positively with g_s and g_m (Supplementary Fig. S6 at *JXB* online). C_i-C_c ranged from 240 to 112 µmol mol^{-1} in woody deciduous and evergreen species, and had lower values (40–67 µmol mol^{-1}) in herbs. C_i-C_c decreased with increasing g_m (Supplementary Fig. S7

at *JXB* online). This relationship was qualitatively identical when g_m was expressed on the leaf area or dry mass basis (data not shown).

g_m in relation to leaf structural and anatomical traits

g_m per dry mass was negatively associated with M_A ($r^2 = 0.85$, $P < 0.0005$; data not shown). g_m per unit leaf area or per unit dry mass (data not shown) was not correlated with S_m/S, reflecting the circumstance that S_m/S was almost invariable, between 16 and 24 $m^2\ m^{-2}$ across the species. S_c/S was not significantly correlated with g_m (Fig. 2A, $P > 0.13$). However, a positive correlation between g_m and S_c/S was observed when the species with the largest T_{cw} (*Pittosporum tobira* and *Q. brantii*) were not included in the correlation ($r^2=0.77$, $P < 0.0001$; data not shown).

The positive and significant correlation ($r^2=0.84$, $P < 0.001$) between g_m and $(S_c/S)/D_L$ suggested the importance of the anatomical components to the internal diffusion of CO_2 (Fig. 2B). Moreover, the negative and significant relationship observed between $g_m/(S_c/S)$ and T_{cw} showed the importance of T_{cw} in affecting g_m (Fig. 2C).

g_m calculated from anatomical variables

Using the leaf anatomical traits measured, g_m was modelled and compared with g_m measured by the method of Harley *et al*. (1992). A good positive linear relationship between modelled and measured g_m was observed ($r^2=0.90$, $P < 0.0001$; Fig. 3). However, the slope was different from unity, so that the g_m modelled tended to be overestimated in species with high M_A and underestimated in species with low M_A. g_m values calculated by the model based on leaf anatomy ranged between 0.217 and 0.056 mol $m^{-2}\ s^{-1}$. *H. annuus* showed the largest and *W. filifera* the smallest values of g_m. The coefficient of intraspecific variation in g_m estimates for different replicates was lower than for the experimental estimations, being between 1.2% (*Betula pubescens*) and 22% (*Pittosporum tobira*).

Overall importance of g_m

According to quantitative limitations analysis of A_N, stomatal openness and g_m restricted the photosynthetic capacity to a similar percentage, 19–65% and 13–64%, respectively. However, the biochemical limitations were lower than the stomatal and mesophyll limitations, being between 6 and 33% (Fig. 4A–C). Both the stomatal and biochemical components tended to be more important in species with non-sclerophytic leaves (low M_A), whilst mesophyll diffusion limitation was most significant in species with high M_A (Fig. 4). Thus, herbaceous plants showed the maximum values for stomatal limitations, whilst the maximum mesophyll limitations were observed in evergreen species with more robust foliage structure.

Limitation of g_m due to individual components of the diffusion pathway

From the different components of the whole diffusion pathway of CO_2, the percentage limitations of g_m were estimated (Fig. 4D–I). Intercellular air spaces represented a smaller resistance to the CO_2 diffusion (4–22%) than the cellular phase, because the rate of CO_2 diffusion in air was larger than in water. In the cellular phase, the cell walls appeared to be the most important factor that limited the internal diffusion of CO_2 in the species that presented a high M_A. However, the plants with low M_A that presented a low percentage of limitation of g_m by the cell wall revealed a higher limitation by the stroma of around 43%. On the other hand, the plasmalemma and chloroplast envelope accounted for only up to 8% of the limitation.

Discussion

Values of g_m in a range of species exhibiting different foliage morphologies

The range of g_m values observed in our study is representative of the whole range of g_m values described so far in large

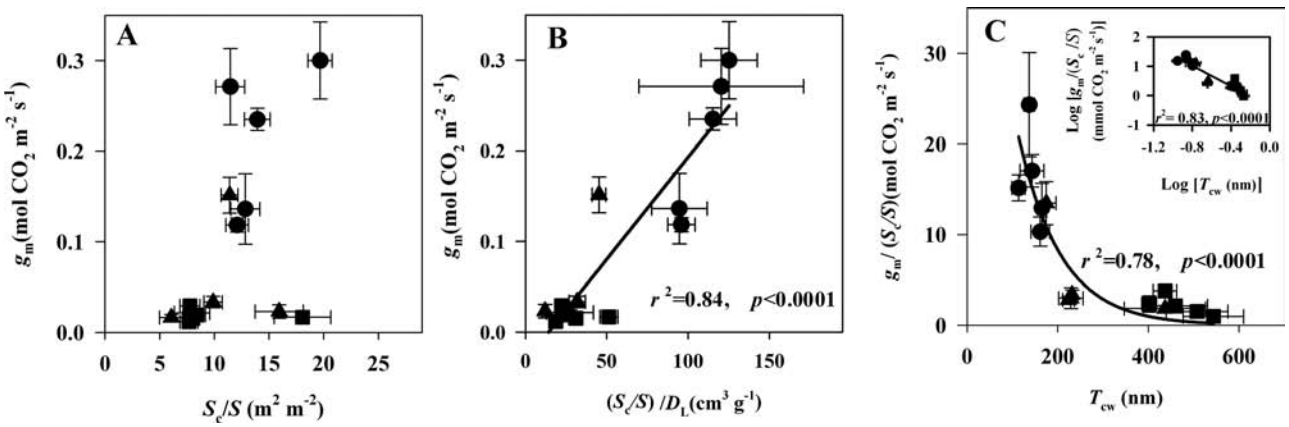

Fig. 2. Correlations of mesophyll diffusion conductance (g_m) determined according to Harley *et al*. (1992) with the surface area of chloroplasts exposed to intercellular airspaces per unit leaf area (S_c/S) (A), mesophyll diffusion conductance with chloroplast surface area per leaf density ($(S_c/S)/D_L$) (B), and mesophyll diffusion conductance per S_c/S ($g_m/(S_c/S)$) with T_{cw} (C). In the main panels, the data were fitted by linear (B) and non-linear (C) regressions in the form $y=ae^{-}bx$. In the inset, the data were fitted by linear regression. Different species are represented as: herbs (circles), woody deciduous and semi-deciduous species (triangles), and woody evergreen species (squares). Values are means ±standard error (SE) of three to four replicates per species.

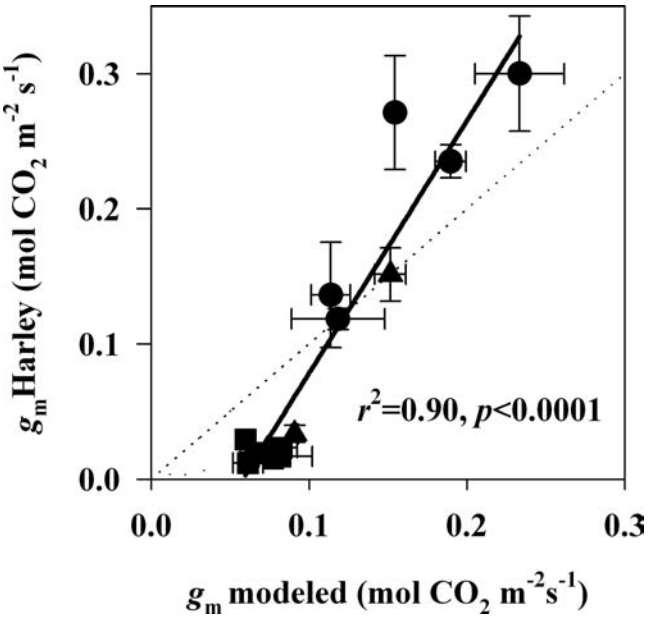

Fig. 3. The relationship between mesophyll diffusion conductance (g_m) measured with Harley *et al.* method and g_m modelled with anatomical parameters (Eqn 6–15). Values are means ±SE of three replicates per species. Symbols are the same as in Fig. 2. The data were fitted by linear regression. Broken lines correspond to the 1:1 relationship.

literature-based datasets, except that the maximum g_m values found in the present study were somewhat lower than reported previously (Flexas *et al.*, 2008; Warren, 2008, Niinemets *et al.*, 2009a). These relatively low maximum values were possibly due to moderate growth light intensity compared with full sun (Piel *et al.*, 2002; Niinemets *et al.*, 2009a). This explanation is consistent with the observations of a significant number of chloroplasts not closely facing the cell walls (Fig. 2A) and relatively low ratios of chloroplast exposed to mesophyll exposed cell wall surfaces (S_c/S_m) (Supplementary Table S4), both being traits that depend on the growth light environment (Terashima *et al.*, 2006).

Relationship of g_m to leaf anatomy and its importance in limiting photosynthesis

As in previous studies, g_m showed a high degree of correlation with several leaf anatomic characteristics, notably a negative correlation with M_A (Flexas *et al.*, 2008; Niinemets *et al.*, 2009a,*b*) and a positive correlation with S_c/S (Evans *et al.*, 1994, 2009). The M_A effect on g_m supports the idea that g_m depends on species differences in leaf density, as density was positively correlated with M_A, whilst leaf thickness showed a weak correlation. The photosynthetic capacity was also significantly and positively correlated with g_m as demonstrated previously (reviewed by Flexas *et al.*, 2008; Niinemets *et al.*, 2009a).Overall, these results suggest that, in species with high M_A, photosynthesis is more limited by g_m, as indirectly supported by the negative effect of leaf density on g_m (Niinemets, 1999) and more directly evidenced by the fact that they present higher values of C_i-C_c (Warren, 2008; Niinemets *et al.*, 2009a).

The relative contribution of g_s, g_m, and photosynthetic biochemistry to total photosynthesis limitation (following Grassi and Magnani, 2005) was variable and depended on leaf structural characteristics, i.e. M_A (Fig.4A–C). At a typical operating CO_2 concentration, the biochemical limitations of photosynthesis decreased from a maximum of approximately 33% at low M_A to minimum values as M_A increased, whilst, in parallel, mesophyll diffusion limitations increased from a minimum of approximately 15% to maximum values up to 65%. Stomatal limitations showed a less clear variation with M_A. Overall, these data demonstrated that species with low M_A showed a notable coordination of the limiting factors for photosynthesis, i.e. they were similarly co-limited by stomatal, mesophyll, and biochemical limitations. In contrast, species with high M_A were mostly limited by mesophyll (on average by 57%) and stomatal (30%) diffusion, and were less limited by biochemistry (13%). This is consistent with the idea that species with thicker and denser leaves, e.g. evergreen trees, are more limited by g_m than species with thinner leaves (Galmés *et al.*, 2007; Niinemets *et al.*, 2011).

Key structural factors regulating differences in g_m between distant leaf structures

The fact that g_m and mesophyll diffusion limitations were strongly correlated with M_A suggested that interspecific variations in g_m are driven by leaf structural characteristics. Among the key structural traits suggested to limit CO_2 diffusion the most are the traits that alter effective diffusion path length and area for diffusion, in particular T_{cw}, and chloroplast distribution along the exposed mesophyll cell wall (Fig. 2; Evans *et al.*, 2009), although the role of other variables, such as leaf porosity, and the path lengths for CO_2 through the plasmalemma and chloroplast envelope membranes, cytosol, and stroma cannot be ruled out (Evans *et al.*, 2009). In the present study, we modelled g_m considering all major leaf structural traits as described by Tosens *et al.* (2012a). A high significant positive correlation between measured and modelled g_m estimates was found (Fig. 3). This correlation supports the view that at least a significant proportion of the interspecific variations in g_m is somehow related to differences in the thickness of the structures involved in CO_2 diffusion, as well as to the number of parallel CO_2 diffusion pathways determined by S_c/S.

Despite the high correlation, the slope of the relationship was not unity, so that the biggest discrepancies between measured and modelled estimates of g_m were found at the higher and lower ends of g_m. A similar discrepancy was observed in different Australian sclerophyll species occurring in the field under different soil nutrients and water availabilities, especially at high values of g_m (Tosens *et al.*, 2012b).

This strong discrepancy between measured and modelled values may arise from the inherent uncertainties associated with both estimates. As for the Harley *et al.* (1992) approach, besides the small variability in the estimates associated with uncertainties in the exact values of R_L and Γ^* (Supplementary Table S3), it has recently been shown that g_m

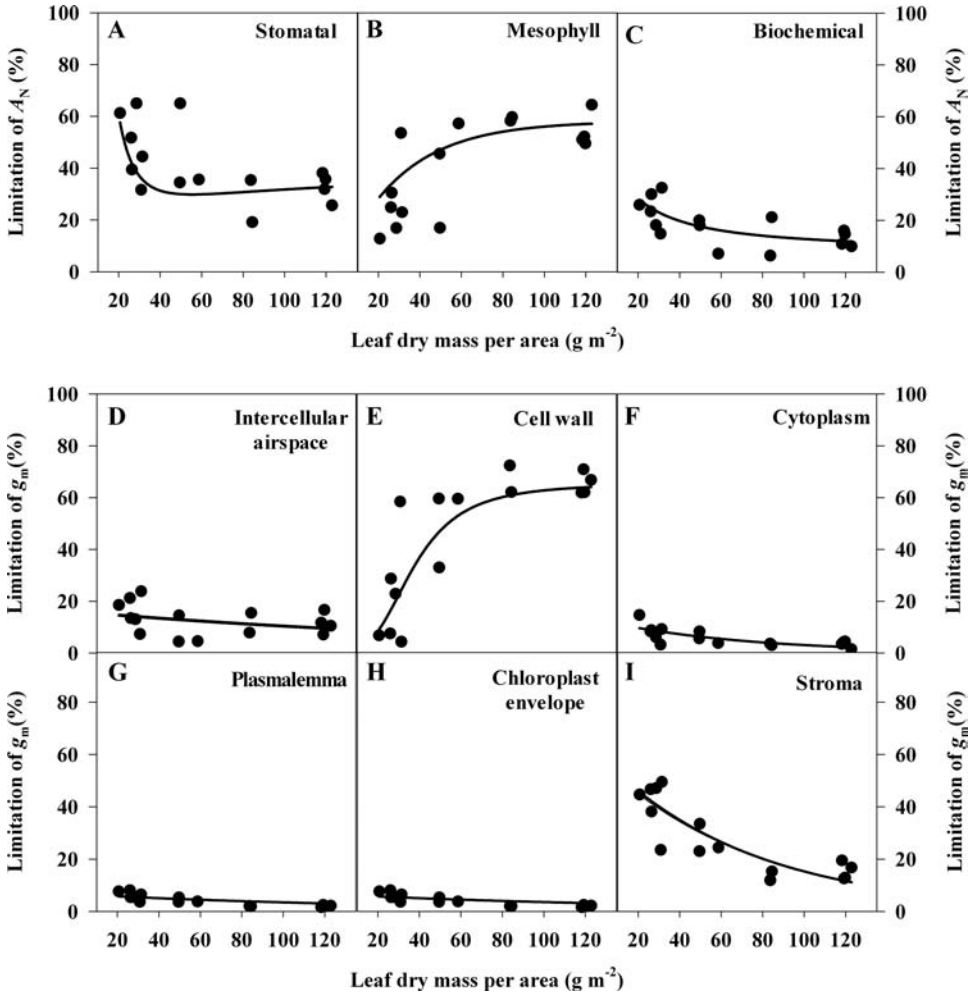

Fig. 4. Quantitative limitation analysis of photosynthetic CO_2 assimilation and mesophyll conductance to CO_2 (g_m) in relation to the leaf dry mass per area (M_A). The stomatal (A), mesophyll (B), and biochemical (C) limitations of photosynthetic assimilation were calculated according to Eqns 16–18. Limitations analyses were based on a chloroplastic CO_2 concentration (C_c) range of 50–100 μmol mol^{-1}. Quantitative limitations of g_m due to different anatomical components of the diffusion pathway were calculated using leaf anatomical characteristics (Eqns 19 and 20). The relative CO_2 diffusion limitations separated were: intercellular spaces (D), cell wall thickness (E), cytoplasm (F), plasmalemma (G), chloroplast envelope (H), and chloroplast stroma (I).

cannot be considered as a purely diffusional component, but instead intrinsically includes a flux-weighted quantity related to the amount of respiratory and photorespiratory CO_2 from the mitochondria diffusing towards the chloroplasts (Tholen *et al.*, 2012). Concerning the anatomically based model used here, the precise outputs largely depend on a number of variables assumed as constants or inferred indirectly. For instance, the reduction in D_w compared with free diffusion in water ($r_{f,i}$) was considered constant for all species, although different for cell wall and intercellular components. Both g_{pl} and g_{env} were also taken as constant, whilst cell wall porosity (p_i) was indirectly estimated from T_{cw} using an empirical equation. There is not sufficient knowledge for the actual values of all these parameters, and they may vary among species, hence contributing to most of the observed slope discrepancy. It can be seen, for instance, that the difference between measured and modelled g_m almost disappeared when the $r_{f,i}$ values were calculated using a least-squares iterative analysis (Supplementary Fig. S2). However, this 'perfect correspondence' is bound to some probably non-realistic $r_{f,i}$ values as low as 0.05. Moreover, values of g_m have been modelled considering CO_2 diffusivities in the different media involved—assumed to be either 'pure' air, lipid, or aqueous phases with fixed thicknesses, whilst, in most cases, determination of the thickness of the given phase is not that straightforward. Also, we assumed no facilitation mechanism that could improve the diffusivities in lipid and aqueous phases. Among these, membrane-bound aquaporins (Uehlein *et al.*, 2003, 2008; Hanba *et al.*, 2004; Flexas *et al.*, 2006) and cytosol and stromal forms of carbonic anhydrases (Price *et al.*, 1994; Gillon and Yakir, 2000) are likely candidates (Terashima *et al.*, 2011). For instance, allowing g_{pl} and/or g_{env} to vary within the range of published values (Evans *et al.*, 2009) also results in a better agreement between the measured and modelled values (Supplementary Fig. S8 at *JXB* online). In summary, current uncertainties about the actual values of these parameters and

their variability among species preclude the development of a truly predictive anatomically based model for g_m. However, the good correlation, despite the divergent slope, can be taken as strong evidence that a substantial part of g_m is indeed dependent on a series of leaf anatomical features.

Despite the discussed limitations of the model approach used here, the results suggest that chloroplast distribution and T_{cw} are the most influential leaf structural characteristics in setting the limits for g_m (Evans *et al.*, 2009; Terashima *et al.*, 2011). In particular, a significant positive correlation was found between g_m and S_c/S only when species with very large T_{cw} (*Q. brantii* and *Pittosporum tobira*) were excluded, highlighting the fact that the impact of chloroplast distribution on g_m became less important as T_{cw} increased, in agreement with past suggestions (Terashima *et al.*, 2006, 2011).

In addition, a highly significant negative relationship was observed between the ratio $g_m/(S_c/S)$ and T_{cw} considering all species, similar to that obtained by Terashima *et al.* (2011) pooling literature data. Using a limitation analysis to separate the contributions of the components of g_m (Eqns 13 and 14) revealed that, globally, the limitation imposed by T_{cw} spanned the most, ranging from approximately 4 to 70% (Fig. 4E). This was followed by chloroplast stroma, which ranged from 4 to 46% (Fig. 4F, I). However, the limitations inside the cell (cytosol and stroma) could be underestimated, especially in species with high M_A, as g_m was modelled assuming that cytosolic and stromal viscosity ($r_{f,i}$) was constant in all species.

The limitations imposed by intercellular air spaces, the plasmalemma, and the chloroplast envelope were much smaller than the rest of the diffusion pathway components as was observed by Tosens *et al.* (2012a,*b*). The fact that the latter two components had only a moderate effect on limiting g_m is in conflict with the observed larger g_m changes observed in aquaporin mutant plants without any appreciable differences in S_c/S or any other leaf structural characteristic (Flexas *et al.*, 2006). This could be due to the fact that the assumed values for g_{pl} and g_{env} are constant among species, which may not necessarily be the case. Differences of up to four orders of magnitude have been reported for CO_2 permeabilities of biological membranes. For instance, if the permeability for a given species was 0.00002 m s^{-1}, as found for chloroplast envelopes by Uehlein *et al.* (2008), instead of the 0.0035 m s^{-1} used in the present simulation, the combined limitation to g_m imposed could be larger than 40% (data not shown). At the other extreme, if values were closer to the 0.016 m s^{-1} reported by Missner *et al.* (2008) for lipid bilayers, the maximum modelled g_m values will be closer to estimates based by the Harley *et al.* (1992) approach (data not shown). Clearly, improved knowledge on the actual permeability to CO_2 of biological membranes is required to fully understand the basis for the regulation of g_m.

Despite these general tendencies, the impact of each specific leaf component on g_m changed with M_A. Specifically, the limitations imposed by T_{cw} strongly increased with increasing M_A, whilst the limitations associated with all the other components decreased with increasing M_A. Thus, in species with low M_A, like annual herbs, about 60% of the total limitation to g_m is imposed by cytoplasm and stroma, whilst another 12% is accounted for by the plasmalemma and chloroplast envelope. Moreover, in species with thinner leaves, the fraction of exposed cell wall lined with chloroplasts ($g_{cel,1}$) was higher, whilst limitations inside the cell through interchoroplastial areas ($g_{cel,2}$) were more important in species with higher M_A (Fig. S9 at *JXB* online). This suggests that it is in such species where facilitating mechanisms (aquaporins, carbonic anhydrases, chloroplast movements, and others) have the strongest influence on g_m. In contrast, in species with high M_A, like evergreen sclerophylls, g_m is mostly (up to 70%) limited by T_{cw}, which is likely to be less variable in the short term, and may explain the low photosynthetic capacity displayed by these plants even under non-limiting conditions. Possible interspecific variation in the role of aquaporins in limiting g_m is clearly a topic that deserves high priority in future studies.

In conclusion, the present study showed that mesophyll limitations are crucial in determining the maximum photosynthetic capacity when a large range of leaf types are analysed collectively. These limitations are variable depending on the leaf structural properties, i.e. M_A and associated structural traits such as leaf density. The variability in mesophyll diffusion limitations was explained mainly by variations in the rate of CO_2 diffusion pathways through cell walls, as well as the area for diffusion determined by the chloroplast distribution. However, the impact of each component of the diffusion pathway largely depended on M_A, so that CO_2 diffusion in species with thin leaves (e.g. herbs) depends more on membranes and aqueous compartments—and is probably more influenced by aquaporins and carbonic anhydrases. In contrast, diffusion in species with thick leaves is almost fully determined by cell wall conductance. Altogether, the variability in g_m with M_A helps explain the worldwide leaf economics spectrum showing a negative dependency between photosynthetic capacity and M_A.

Supplementary data

Supplementary data can be found at *JXB* online.

Supplementary Table S1. List of studied species, species origin, life form, and leaf longevity.

Supplementary Table S2. Physiological characteristics measured in all studied species.

Supplementary Table S3. Sensitivity analysis of the influence of uncertainties in chloroplastic hypothetical CO_2 compensation point (Γ*) and day respiration on the estimation of mesophyll conductance (g_m).

Supplementary Table S4. Leaf dry mass per unit area (M_A), leaf thickness (T_L), leaf density (D_L), thickness of mesophyll layers, number of palisade cell layers, mesophyll surface area exposed to intercellular airspace (S_m/S), chloroplast surface area exposed to intercellular airspace (S_c/S), and the ratio S_c/S_m in all studied species.

Supplementary Table S5. Cell wall thickness (T_{cw}), cytoplasm thickness (T_{cyt}), chloroplasts length (L_{chl}), chloroplasts thickness (T_{chl}), and effective porosity of the cell wall (p_i).

Supplementary Fig. S1. Representative light micrographs at 200× magnification for *Phaseolus vulgaris*, *Ficus elastica*,

and *Washingtonia filifera*, and representative transmission electron micrographs at 2000× magnification for *Helianthus annuus*, *Acer negundo*, and *Washingtonia filifera* and at 20 000× magnification for *H. annuus*, *Alnus subcordata* and *Pittosporum tobira*.

Supplementary Fig. S2. The relationship between mesophyll diffusion conductance (g_m) measured with the Harley Harley *et al*. (1992) method and g_m modelled with anatomical parameters using least-squares iterative analysis for the $r_{f,i}$ parameter.

Supplementary Fig. S3. Effects of the parameter $r_{f,i}$ of the cytosol and chloroplast stroma on g_m modelled from anatomical characteristics.

Supplementary Fig. S4. Correlation between leaf density (D_L) and leaf dry mass per unit area (M_A).

Supplementary Fig. S5. Relationship between g_m measured according to Harley *et al*. (1992) method versus the Ethier and Livingston (2004) method.

Supplementary Fig. S6. Net photosynthesis rate (A_N) in relation to stomatal (g_s) and mesophyll (g_m) conductance.

Supplementary Fig. S7. The relationship between g_m and CO_2 drawdown (C_i-C_c).

Supplementary Fig. S8. The relationship between mesophyll diffusion conductance (g_m) measured with the Harley *et al*. (1992) method and g_m modelled with anatomical parameters using different values for the membrane permeabilities of plasmalemma (g_{pl}) and chloroplast membrane (g_{env}) conductances.

Supplementary Fig. S9. Quantitative limitation analysis of conductance to CO_2 inside the cell ($g_{cel,tot}$) calculated on the basis of leaf anatomical characteristics.

Acknowledgements

The authors are grateful to Mª Teresa Mínguez, Universitat de València (Sección Microscopia Electrónica, SCSIE) and Dr Ferran Hierro and Maria Pocoví, Universitat de les Illes Balears (Serveis Cientifico-Tècnics) for technical support during microscopic analyses. This work has been developed with financial support from the Spanish Ministry of Science and Technology Projects AGL2008-04525-C02-01, BFU2008-01072 (MEFORE), and BFU2011-23294 (MECOME) and a pre-doctoral fellowship of the programme JAE (CSIC) to M.T., the Estonian Ministry of Science and Education (institutional grant IUT8-3), the European Commission through European Regional Fund (the Estonian Center of Excellence in Environmental Adaptation), and a post-doctoral grant (MJD122) supported by the European Social Fund programme Mobilitas, as well as scientific cooperation between the Estonian Academy of Sciences and the CSIC (2009EN0005).

References

Bernacchi CJ, Portis AR, Nakano H, von Caemmerer S, Long SP. 2002. Temperature response of mesophyll conductance. Implications for the determination of Rubisco enzyme kinetics and for limitations to photosynthesis *in vivo*. *Plant Physiology* **130,** 1992–1998.

Bernacchi CJ, Singsaas EL, Pimentel C, Portis AR, Long SP. 2001. Improved temperature response functions for models of Rubisco-limited photosynthesis. *Plant, Cell & Environment* **24,** 253–259.

Ethier GH, Livingston NJ. 2004. On the need to incorporate sensitivity to CO_2 transfer conductance into the Farquhar–von Caemmerer–Berry leaf photosynthesis model. *Plant, Cell & Environment* **27,** 137–153.

Evans JR, von Caemmerer S, Setchell BA, Hudson GS. 1994. The relationship between CO_2 transfer conductance and leaf anatomy in transgenic tobacco with a reduced content of Rubisco. *Australian Journal of Plant Physiology* **21,** 475–495.

Evans JR, Vogelmann TC. 2006. Photosynthesis within isobilateral *Eucalyptus pauciflora* leaves. *New Phytologist* **171,** 171–182.

Evans JR, Kaldenhoff R, Genty B, Terashima I. 2009. Resistances along the CO_2 diffusion pathway inside leaves. *Journal of Experimental Botany* **60,** 2235–2248.

Farquhar GD, von Caemmerer S, Berry JA. 1980. A biochemical model of photosynthetic CO_2 assimilation in leaves of C_3 species. *Planta* **149,** 78–90.

Flexas J, Ribas-Carbó M, Hanson DT, Bota J, Otto B, Cifre J, McDowell N, Medrano H, Kaldenhoff R. 2006. Tobacco aquaporin NtAQP1 is involved in mesophyll conductance to CO_2 *in vivo*. *The Plant Journal* **48,** 427–439.

Flexas J, Díaz-Espejo A, Berry JA, Galmés J, Cifre J, Kaldenhoff R, Medrano H and Ribas-Carbó M. 2007. Leakage in leaf chambers in open gas exchange systems: quantification and its effects in photosynthesis parameterization. *Journal of Experimental Botany* **58,** 1533–1543.

Flexas J, Ribas-Carbó M, Diaz-Espejo A, Galmés J, Medrano H. 2008. Mesophyll conductance to CO_2: current knowledge and future prospects. *Plant, Cell & Environment* **31,** 602–621.

Flexas J, Barbour MM, Brendel O, *et al.*. 2012. Mesophyll diffusion conductance to CO_2: an unappreciated central player in photosynthesis. *Plant Science* 193–194, 70–84.

Gallé A, Flórez-Sarasa I, Tomás M, Pou A, Medrano H, Ribas-Carbó M, Flexas J. 2009. The role of mesophyll conductance during water stress and recovery in tobacco (*Nicotiana sylvestris*): Acclimation or limitation? *Journal of Experimental Botany* **60,** 2379–2390.

Galmés J, Flexas J, Keys AJ, Cifre J, Mitchell RAC, Madgwick PJ, Haslam RP, Medrano H, Parry MAJ. 2005. Rubisco specificity factor tends to be larger in plant species from drier habitats and in species with persistent leaves. *Plant, Cell & Environment* **28,** 571–579.

Galmés J, Medrano H, Flexas J. 2007. Photosynthetic limitations in response to water stress and recovery in Mediterranean plants with different growth forms. *New Phytologist* **175,** 81–93.

Genty B, Briantais JM, Baker NR. 1989. The relationship between the quantum yield of photosynthetic electron transport and quenching of chlorophyll fluorescence. *Biochimica et Biophysica Acta* **990,** 87–92.

Gillon JS, Yakir D. 2000. Internal conductance to CO_2 diffusion and $C^{18}OO$ discrimination in C_3 leaves. *Plant Physiology* **123,** 201–213.

Grassi G, Magnani F. 2005. Stomatal, mesophyll conductance and biochemical limitations to photosynthesis as affected by drought and

leaf ontogeny in ash and oak trees. *Plant, Cell & Environment* **28,** 834–849.

Hanba YT, Shibasaka M, Hayashi Y, Hayakawa T, Kasamo K, Terashima I, Katsuhara M. 2004. Overexpression of the barley aquaporin HvPIP2;1 increases internal CO_2 conductance and CO_2 assimilation in the leaves of transgenic rice plants. *Plant & Cell Physiology* **45,** 521–529.

Harley PC, Loreto F, Di Marco G, Sharkey TD. 1992. Theoretical considerations when estimating the mesophyll conductance to CO_2 flux by the analysis of the response of photosynthesis to CO_2. *Plant Physiology* **98,** 1429–1436.

Hassiotou F, Renton M, Ludwig M, Evans JR, Veneklaas EJ. 2010. Photosynthesis at an extreme end of the leaf trait spectrum: how does it relate to high leaf dry mass per area and associated structural parameters? *Journal of Experimental Botany* **61,** 3015–3028.

Hikosaka K, Shigeno A. 2009. The role of Rubisco and cell walls in the interspecific variation in photosynthetic capacity. *Oecologia* **160,** 443–451.

Jones H.G. 1985. Partitioning stomatal and non-stomatal limitations to photosynthesis. *Plant, Cell & Environment* **8,** 95–104.

Loreto F, Di Marco G, Tricoli D, Sharkey TD. 1994. Measurements of mesophyll conductance, photosynthetic electron transport and alternative electron sinks of field-grown wheat leaves. *Photosynthesis Research* **41,** 397–403.

Loreto F, Tsonev T, Centritto M. 2009. The impact of blue light on leaf mesophyll conductance. *Journal of Experimental Botany* **60,** 2283–2290.

Missner A, Kugler P, Saparov SM, Sommer K, Mathai JC, Zeidel ML, Pohl P. 2008. Carbon dioxide transport through membranes. *Journal of Biological Chemistry* **283,** 25340–25347.

Niinemets Ü. 1999. Components of leaf dry mass per area—thickness and density—alter leaf photosynthetic capacity in reverse directions in woody plants. *New Phytologist* , **144,** 35–47.

Niinemets Ü. 2001. Global-scale climatic controls of leaf dry mass per area, density, and thickness in trees and shrubs. *Ecology* **82,** 453–469.

Niinemets Ü, Cescatti A, Rodeghiero M, Tosens T. 2005. Leaf internal diffusion conductance limits photosynthesis more strongly in older leaves of Mediterranean evergreen broad-leaved species. *Plant, Cell & Environment* **28,** 1552–1566.

Niinemets U, Cescatti A, Rodeghiero M, Tosens T. 2006. Complex adjustments of photosynthetic potentials and internal diffusion conductance to current and previous light availabilities and leaf age in Mediterranean evergreen species *Quercus ilex*. *Plant, Cell & Environment* **29,** 1159–1178.

Niinemets Ü, Díaz-Espejo A, Flexas J, Galmés J, Warren CR. 2009*a*. Role of mesophyll diffusion conductance in constraining potential photosynthetic productivity in the field. *Journal of Experimental Botany* **60,** 2249–2270.

Niinemets Ü, Flexas J, Peñuelas J. 2011. Evergreens favored by higher responsiveness to increased CO_2. *Trends in Ecology & Evolution* **26,** 136–142.

Niinemets Ü, Portsmuth A, Tena D, Tobias M, Martesanz S, Valladares F. 2007. Do we underestimate the importance of leaf size in plant economics? Disproportional scaling of support costs within the spectrum of leaf physiognomy. *Annals of Botany* **100,** 283–303.

Niinemets Ü, Reichstein M. 2003*a*. Controls on the emission of plant volatiles through stomata: a sensitivity analysis. *Journal of Geophysical Research—Atmospheres* **108,** 4211, doi:10.1029/2002JD002626.

Niinemets Ü, Reichstein M. 2003*b*. Controls on the emission of plant volatiles through stomata: Differential sensitivity of emission rates to stomatal closure explained. *Journal of Geophysical Research* , **108,** 4208.

Niinemets Ü, Wright IJ, Evans JR. 2009*b*. Leaf mesophyll diffusion conductance in 35 Australian sclerophylls covering a broad range of foliage structural and physiological variation. *Journal of Experimental Botany* **60,** 2433–2449.

Nobel PS. 1991. *Physicochemical and environmental plant physiology* , 4th edn. San Diego, CA: Academic Press.

Parkhurst DF, Mott KA. 1990. Intercellular diffusion limits to CO_2 uptake in leaves: studies in air and helox. *Plant Physiology* **94,** 1024–1032.

Peguero-Pina JJ, Flexas J, Galmés J, Sancho-Knapik D, Barredo G, Villarroya D, Gil-Pelegrín E. 2012. Leaf anatomical properties in relation to differences in mesophyll conductance to CO_2 and photosynthesis in two related Mediterranean *Abies* species. *Plant, Cell & Environment* **35,** 2121–2129

Piel C, Frak E, Le Roux X, Genty B. 2002. Effect of local irradiance on CO_2 transfer conductance of mesophyll in walnut. *Journal of Experimental Botany* **53,** 2423–2430.

Price D, von Caemmerer S, Evans JR, Yu JW, Lloyd J, Oja V, Kell P, Harrison K, Gallagher A, Badger M. 1994. Specific reduction of chloroplast carbonic anhydrase activity by antisense RNA in transgenic tobacco plants has a minor effect on photosynthetic CO_2 assimilation. *Planta* **193,** 331–340.

Rondeau-Mouro C, Defer D, Leboeuf E, Lahaye M. 2008. Assessment of cell wall porosity in *Arabidopsis thaliana* by NMR spectroscopy. *International Journal of Biological Macromolecules* **42,** 83–92.

Scafaro AP, Von Caemmerer S, Evans JR, Atwell B. 2011. Temperature response of mesophyll conductance in cultivated and wild Oryza species with contrasting mesophyll cell wall thickness. *Plant, Cell & Environment* **34,** 1999–2008.

Syvertsen JP, Lloyd J, McConchie C, Kriedemann PE, Farquhar GD. 1995. On the relationship between leaf anatomy and CO_2 diffusion through the mesophyll of hypostomatous leaves. *Plant, Cell & Environment* **18,** 149–157.

Terashima I, Hanba YT, Tazoe Y, Vyas P, Yano S. 2006. Irradiance and phenotype: comparative eco-development of sun and shade leaves in relation to photosynthetic CO_2 diffusion. *Journal Experimental Botany* **57,** 343–354.

Terashima I, Hanba YT, Tholen D, Niinemets Ü. 2011. Leaf functional anatomy in relation to photosynthesis. *Plant Physiology* **155,** 108–116.

Thain JF. 1983. Curvature correlation factors in the measurements of cell surface areas in plant tissues. *Journal of Experimental Botany* **34,** 87–94.

Tholen D, Boom C, Noguchi K, Ueda S, Katase T, Terashima I. 2008. The chloroplast avoidance response decreases internal conductance to CO_2 diffusion in *Arabidopsis thaliana* leaves. *Plant, Cell and Environment* **31,** 1688–1700.

Tholen D, Ethier G, Genty B, Pepin S, Zhu X. 2012. Variable mesophyll conductance revisited: theoretical background and experimental implications. *Plant, Cell & Environment* **35,** 2087–2103.

Tosens T, Niinemets Ü, Vislap V, Eichelmann H, Castro-Díez P. 2012*a*. Developmental changes in mesophyll diffusion conductance and photosynthetic capacity under different light and water availabilities in *Populus tremula*: how structure constrains function. *Plant, Cell & Environment* **35,** 839–856

Tosens T, Niinemets Ü, Westoby M, Wright IJ. 2012*b*. Anatomical basis of variation in mesophyll resistance in eastern Australian sclerophylls: news of a long and winding path. *Journal of Experimental Botany* **63,** 5105–5119.

Uehlein N, Lovisolo C, Siefritz F, Kaldenhoff R. 2003. The tobacco aquaporin NtAQP1 is a membrane CO_2 pore with physiological functions. *Nature* **425,** 734–737.

Uehlein N, Otto B, Hanson DT, Fischer M, McDowell N, Kaldenhoff R. 2008. Function of Nicotiana tabacum aquaporins as chloroplast gas pores challenges the concept of membrane CO_2 permeability. *Plant Cell* **20,** 648–657.

Warren C. 2008. Stand aside stomata, another actor deserves centre stage: the forgotten role of the internal conductance to CO_2 transfer. *Journal Experimental Botany* **59,** 1475–1487.

Wright IJ, Reich PB, Westoby M, *et al.*., 2004. The world-wide leaf economics spectrum. *Nature* **428,** 821–827.